Single Baseline 3-D Structure Retrieval Using Radar with Wide Fractional Bandwidth Mounted on Drones

Sumin Kim[a], Víctor Mustieles Pérez[a, b], Gerhard Krieger[a], and Michelangelo Villano[a]
[a]German Aerospace Center (DLR), Münchener Straße 20, 82234 Weßling, Germany
[b]Friedrich-Alexander-Universität (FAU), Martens Straße 5a, 91058, Erlangen, Germany

Abstract

Synthetic aperture radar (SAR) interferometry (InSAR) provides accurate topographic information of an area by using of a pair of SAR images. However, ambiguities arise in the case of volumetric media where multiple scattering occur in a single resolution cell. Polarimetry-based methods assume orthogonal and deterministic scattering mechanisms to resolve the ambiguity and obtain three-dimensional structure of the volume. SAR tomography use additional measurements which require numerous observations. An alternative approach is to use signals with wide fractional bandwidth and obtain the InSAR coherence over a wide range of vertical wavenumber with a single baseline. Signals with a wide fractional bandwidth is available from radars mounted on drones, which is a promising platform for local and frequent SAR remote sensing. A method to simulate radar data backscattered from semi-transparent media and the coherence estimation over a wide vertical wavenumber using a single baseline is presented. The coherence estimated from the simulated data can be used to demonstrate the single-baseline three-dimensional inversion method.

1 Introduction

While synthetic aperture radar (SAR) interferometry is a precise method to map the Earth's surface, ambiguities arise for volumetric media where multiple scattering occur in a single resolution cell [1]. Attempts were made to resolve these ambiguities using additional measurements and processing for measuring above ground biomass [2, 3], forest height retrieval [4, 5], and agricultural monitoring [6].

Polarimetric InSAR (PolInSAR) employ InSAR data from multiple polarimetric channels to separate different scattering mechanisms occurring at different heights [7, 8]. These methods are effective for forest height retrieval, where the assumption that orthogonal scattering mechanisms occur at different heights is valid.

Methods that use SAR data from multiple acquisitions in different heights exploit the Fourier relationship between the data and vertical reflectivity [9, 10] or the InSAR coherence, which can be modeled according to the vertical scattering profile [11, 12]. However, these methods require tens of acquisitions in the vertical direction to properly acquire the volumetric information. The vertical wavenumber k_z, which is the ratio between geometric parameters of an InSAR acquisition, is a factor used to model the the InSAR coherence. Due to the narrow fractional bandwidth used in conventional radar systems, diverse measurement in the vertical wavenumber is only possible using multiple acquisitions. These acquisitions require immense effort in data acquisition and may lead to temporal decorrelation.

While the narrowband signals cannot be avoided in airborne or spaceborne radars due to regulations, transmit signals with frequency spanning over L-, S-, and C-bands are being investigated for use in radars mounted on drones or unmanned aerial vehicles (UAVs) [13, 14]. These radars with a wide fractional bandwidth enable the measurement over a wide range of vertical wavenumber using a single baseline, which can be exploited to invert the three-dimensional information of a semi-transparent medium [15]. A high-level overview of the single baseline inversion scheme is depicted in **Figure 1**.

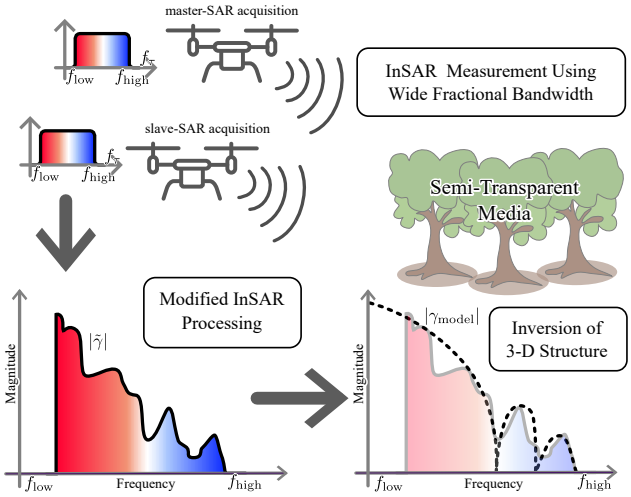

Figure 1 A high-level overview of the method to retrieve three-dimensional information using a single baseline.

In this work, the InSAR coherence is estimated over a wide range of vertical wavenumber assuming a radar mounted on a drone. The radar is assumed to transmit signals with a wide fractional bandwidth where the ratio between the bandwidth and center frequency is larger than one. Point scatterers that model a semi-transparent media were used to generate the simulated radar data. The InSAR

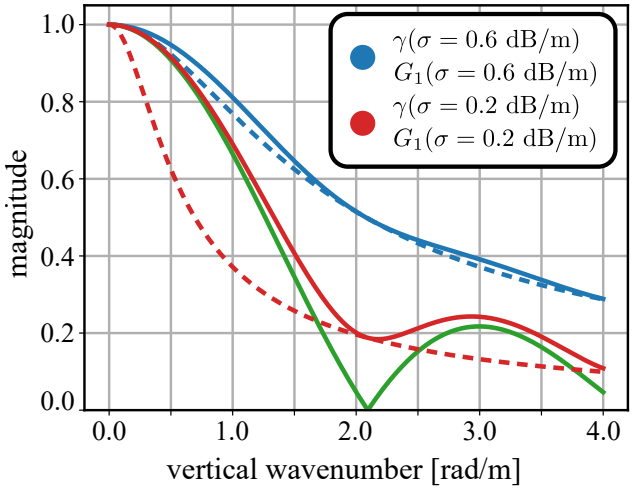

Figure 2 InSAR coherence model assuming a random volume with constant extinction coefficient. The solid blue and red lines depict the coherence varying with different wavenumbers for extinction coefficient of 0.6 dB/m and 0.2 dB/m, respectively. The dashed lines depict the factor of convolution that involves the extinction coefficient. The blue line depicts the factor of convolution that involves the volume height.

data of a single baseline was processed to estimate the coherence over a wide range of vertical wavenumber and was compared with the expected coherence.

2 Vertical Scattering Profile and Coherence Model

The InSAR coherence is a normalized complex correlation coefficient between a pair of SAR images. While the phase of InSAR coherence is used to extract the topographic information, the magnitude involves the quality of the height measurement. The magnitude of InSAR coherence decrease in the presence of semi-transparent media due to multiple scattering from different heights, resulting in the loss of height measurement accuracy. Treuhaft et al. showed that the coherence due to volumetric scattering can be modeled as follows:

$$\begin{aligned}\gamma &= \exp\left[j\phi_0(z_0)\right]\frac{\int_0^{h_v}\exp\left(j\frac{4\pi B_\perp}{cR_s\sin\theta}fz\right)g_v(z)\,dz}{\int_0^{h_v}g_v(z)\,dz}\\ &= \exp\left[j\phi_0(z_0)\right]\frac{\int_0^{h_v}\exp\left(jk_z z\right)g_v(z)\,dz}{\int_0^{h_v}g_v(z)\,dz},\end{aligned} \tag{1}$$

where j is the unit imaginary number, $\phi_0(z_0)$ is the topographic phase with regards to the ground z_0, $B_\perp$ is the perpendicular baseline, c is the speed of light, θ is the incidence angle, f is the frequency, z is the height from the ground, and $g_v(z)$ is the vertical scattering profile [16].

In (1), the vertical wavenumber k_z is defined as a ratio of geometric parameters written as follows:

$$k_z = \frac{4\pi B_\perp}{cR_s\sin\theta}f. \tag{2}$$

Given that signals with wide fractional bandwidth is available, the change in the frequency f is considerable and the coherence can be modeled as a continuous function of vertical wavenumber.

Assuming a constant extinction with depth, the vertical scattering profile can be written using two parameters h_v and σ as follows:

$$g_v(z) = \exp\left[\frac{\sigma}{\cos\theta}\right]\mathrm{rect}\left[\frac{z-h_v/2}{h_v}\right], \tag{3}$$

where h_v and σ is the volume height and the two-way extinction coefficient. The function rect is a window function defined in the interval as $\mathrm{rect}(\cdot) = 1$ if $-1/2 < \cdot \leq 1/2$ and zero elsewhere.

The coherence model for a vertical scattering profile with a constant extinction can be derived using (1) and (3) as follows:

$$|\gamma(k_z)| = \frac{\sigma}{\cos\theta}\left|\frac{G_1(k_z;\sigma) * \left(\exp\left[j\frac{h_v}{2}k_z\right]\mathrm{sinc}\left[\frac{h_v}{2\pi}k_z\right]\right)}{1-g_1(-h_v;\sigma)}\right|, \tag{4}$$

where $*$ denote the convolution operator and sinc is defined as $\mathrm{sinc}(\cdot) = \sin(\pi\cdot)/(\pi\cdot)$. In (4), g_1 and G_1 is the vertical scattering profile assuming an infinite volume height and it's Fourier transform written as follows:

$$\begin{aligned}g_1(z;\sigma) &= \exp\left[\frac{\sigma}{\cos\theta}z\right] \quad \text{if } z\in(-\infty,0]\\ G_1(k_z;\sigma) &= \frac{\int_{-\infty}^{\infty}\exp\left(jk_z z\right)g_1(z;\sigma)\,dz}{\int_{-\infty}^{\infty}g_1(z;\sigma)\,dz}\\ &= \frac{1}{1+j\frac{k_z}{\sigma/\cos\theta}}\end{aligned} \tag{5}$$

An example of the coherence model assuming a volume height of 3 m is depicted in **Figure 2** as solid blue and red lines. The two coherence models differ in the value of extinction coefficient, where the blue and red line represent the result from $\sigma = 0.6$ dB and $\sigma = 0.2$ dB/m, respectively. The function G_1 corresponding to the two extinction coefficients are depicted in dashed lines, and the sinc-function in (4) is depicted in a green line. It is shown that for higher extinction coefficients, the expected coherence is no longer similar to the sinc-function, which involve the volume height parameter.

The simulated radar data were generated assuming a semi-transparent media with constant extinction coefficient $\sigma = 0.5$ dB/m, constant volume height $h_v = 3$ m, and flat ground topography $z_0 = 0$ m. The slave acquisition was assumed to be 3 m away from the master acquisition in the direction perpendicular to the line of sight.

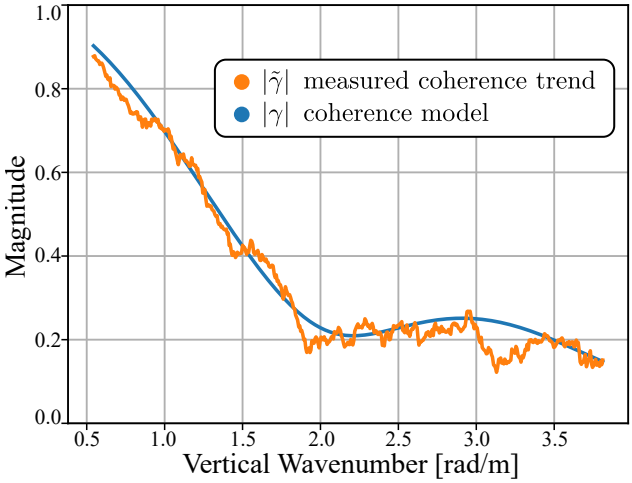

Figure 3 Coherence trend estimated from simulated data (orange) and the coherence model.

The radar data was first filtered in fast time frequency using highly overlapped filters to estimate the coherence change with the vertical wavenumber. The coherence was estimated using a window of 14 looks in azimuth and 14 looks in slant range. The coherence measured using the simulated radar data is depicted in **Figure 3** as solid orange line.

The coherence model calculated using the known volume parameters is depicted in **Figure 3** as solid blue line. The coherence model and the measured coherence exhibit great similarity. Such similarity between the model and the measurement can be used to invert the volumetric parameters of a given resolution cell.

3 Coherence Estimated from Drone-borne InSAR Data

A repeat-pass InSAR experiment was conducted using a ground-penetrating radar operating at L-, S-, and C-band mounted on a hex-rotor UAV. The experiment scene consisted of a flat ground with multiple trihedral corner reflectors and short grass with height less than 50 cm. The antenna illuminated the ground at 45° look angle with no squint.

The radar utilized frequency-modulated continuous-wave (FMCW) waveform with a center frequency, bandwidth, and pulse duration of 2.5 GHz, 3 GHz, and 3.5 ms. The FMCW signal was digitized using a sampling frequency of 2.6 MHz which allowed maximum range of 90 m after range compression.

The experiment incorporated the use of real-time kinematic (RTK) system with a local RTK station on site. The positions were given in local East-North-up (ENU) coordinates referenced to the RTK station, which were used to form the SAR images using back-projection algorithm.

The synthesized SAR image is shown on the left-hand side of Fig. 4, where the vertical and horizontal axes represent the North and East from the RTK station, respectively. The direction of the platform movement was approximately in the negative East direction.

The pair of SAR images were filtered in spatial frequency domain using a two-dimensional filter to obtain the portion of spectrum which represent the response from a specific center frequency. The filtered data was used to estimate the coherence with respect to frequency where the magnitude is shown on the right-hand side of Fig. 4.

4 Outlook

A method to simulate a radar data backscattered from a semi-transparent media is presented in this paper. Assuming a radar signal with a wide fractional bandwidth, the InSAR coherence over a wide vertical wavenumber can be obtained using a single baseline. The vertical scattering profile can be inverted from this measurement subject to it's relationship between the InSAR coherence model. The method to simulate the radar data involves defining the amplitude and phase modulation terms for each point scatterers. The amplitude modulation term is defined based on the vertical coordinate, ground terrain, volumetric parameters, and the vertical scattering profile, which can be used to simulate complex terrain with semi-transparent volume. The simulated radar data were used to obtain the coherence over a wide range of vertical wavenumber. These measurements capable of inverting the volumetric parameters provide an opportunity to achieve three-dimensional structure retrieval without the need of numerous acquisitions.

5 Acknowledgments

This work was partially funded by the European Union (ERC, DRITUCS, 101076275). Views and opinions expressed are however those of the authors only and do not necessarily reflect those of the European Union or the European Research Council Executive Agency. Neither the European Union nor the granting authority can be held responsible for them. This work was co-funded by the Deutsche Forschungsgemeinschaft (DFG, German Research Foundation) GRK 2680 – Project-ID 437847244.

6 Literature

[1] R. Bamler and P. Hartl, "Synthetic aperture radar interferometry," *Inverse Problems*, vol. 14, 01 1998.

[2] E. Blomberg, L. M. H. Ulander, S. Tebaldini, and L. Ferro-Famil, "Evaluating P-band TomoSAR for biomass retrieval in boreal forest," *IEEE Transactions on Geoscience and Remote Sensing*, vol. 59, no. 5, pp. 3793–3804, 2021.

[3] S. Quegan, T. Le Toan, J. Chave, J. Dall, J.-F. Exbrayat, D. H. T. Minh, M. Lomas, M. M. D'Alessandro, P. Paillou, K. Papathanassiou, F. Rocca, S. Saatchi, K. Scipal, H. Shugart, T. L. Smallman, M. J. Soja, S. Tebaldini, L. Ulander, L. Villard, and M. Williams, "The european space agency BIOMASS mission: Measuring forest above-

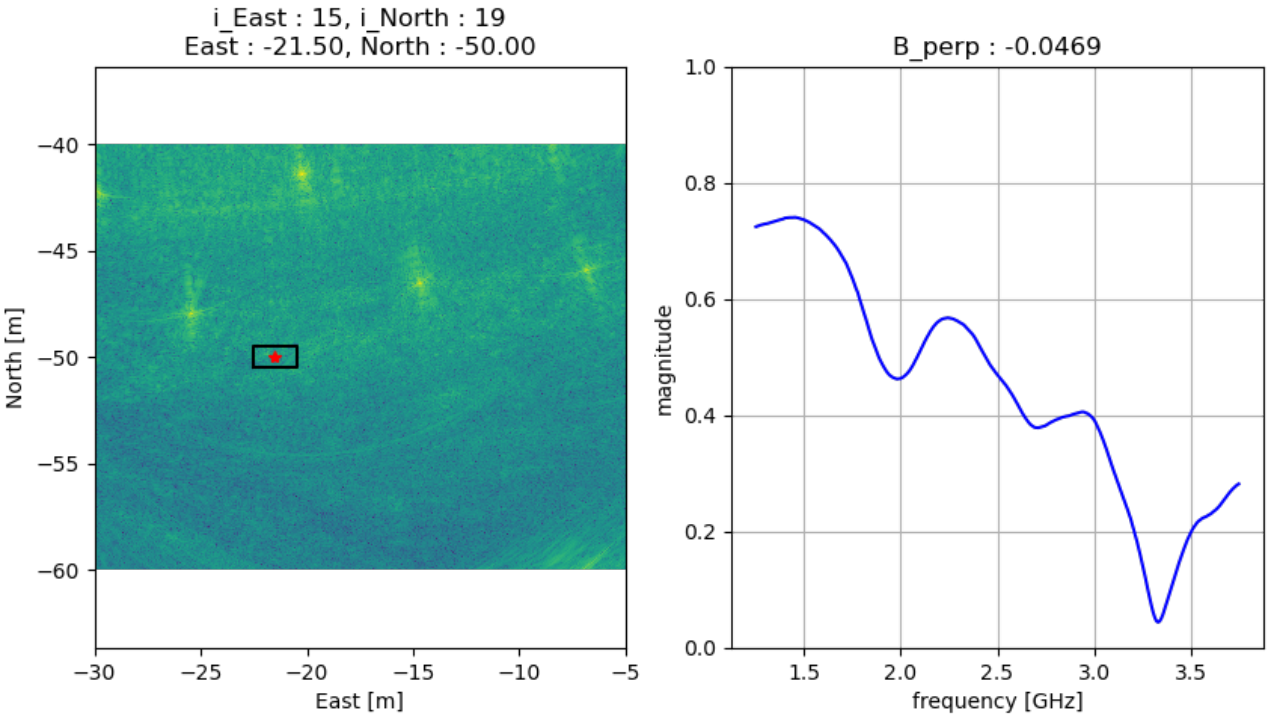

Figure 4 Amplitude image of the SAR image (left) and the magnitude of coherence estimated with respect to frequency.

ground biomass from space," *Remote Sensing of Environment*, vol. 227, pp. 44–60, 2019.

[4] F. Garestier, P. C. Dubois-Fernandez, and K. P. Papathanassiou, "Pine forest height inversion using single-pass X-band PolInSAR data," *IEEE Transactions on Geoscience and Remote Sensing*, vol. 46, no. 1, pp. 59–68, 2008.

[5] I. Hajnsek, F. Kugler, S.-K. Lee, and K. P. Papathanassiou, "Tropical-forest-parameter estimation by means of Pol-InSAR: The INDREX-II campaign," *IEEE Transactions on Geoscience and Remote Sensing*, vol. 47, no. 2, pp. 481–493, 2009.

[6] H. Joerg, M. Pardini, I. Hajnsek, and K. P. Papathanassiou, "3-D scattering characterization of agricultural crops at C-band using SAR tomography," *IEEE Transactions on Geoscience and Remote Sensing*, vol. 56, no. 7, pp. 3976–3989, 2018.

[7] S. Cloude and K. Papathanassiou, "Three-stage inversion process for polarimetric SAR interferometry," *IEE Proceedings - Radar, Sonar and Navigation*, vol. 150, pp. 125–134(9), June 2003.

[8] S. Cloude and K. Papathanassiou, "Polarimetric sar interferometry," *IEEE Transactions on Geoscience and Remote Sensing*, vol. 36, no. 5, pp. 1551–1565, 1998.

[9] A. Reigber and A. Moreira, "First demonstration of airborne SAR tomography using multibaseline L-band data," *IEEE Transactions on Geoscience and Remote Sensing*, vol. 38, no. 5, pp. 2142–2152, 2000.

[10] S. Kim, J. Kim, C. Chung, and M.-H. Ka, "Derivation and validation of three-dimensional microwave imaging using a W-band MIMO radar," *IEEE Transactions on Geoscience and Remote Sensing*, vol. 60, pp. 1–16, 2022.

[11] S. R. Cloude, "Dual-baseline coherence tomography," *IEEE Geoscience and Remote Sensing Letters*, vol. 4, no. 1, pp. 127–131, 2007.

[12] S. Tebaldini, "Single and multipolarimetric SAR tomography of forested areas: A parametric approach," *IEEE Transactions on Geoscience and Remote Sensing*, vol. 48, no. 5, pp. 2375–2387, 2010.

[13] R. Bähnemann, N. R. J. Lawrance, L. Streichenberg, J. J. Chung, M. Pantic, A. Grathwohl, C. Waldschmidt, and R. Y. Siegwart, "Under the sand: Navigation and localization of a micro aerial vehicle for landmine detection with ground-penetrating synthetic aperture radar," *Field Robotics*, 2021.

[14] R. Burr, M. Schartel, A. Grathwohl, W. Mayer, T. Walter, and C. Waldschmidt, "UAV-borne FMCW InSAR for focusing buried objects," *IEEE Geoscience and Remote Sensing Letters*, vol. 19, pp. 1–5, 2022.

[15] S. Kim, V. M. Pérez, G. Krieger, and M. Villano, "Three-dimensional structure inversion through wide fractional bandwidth, UAV-based SAR interferometry," in *2023 24th International Radar Symposium (IRS)*, pp. 1–10, 2023.

[16] R. N. Treuhaft, S. N. Madsen, M. Moghaddam, and J. J. v. Zyl, "Vegetation characteristics and underlying topography from interferometric radar," *Radio Science*, vol. 31, no. 6, pp. 1449–1485, 1996.